PERGAMON

International Journal of Solids and Structures 39 (2002) 2299–2322

INTERNATIONAL JOURNAL OF SOLIDS and STRUCTURES

www.elsevier.com/locate/ijsolstr

Elastic flexural-torsional buckling of continuously restrained arches

Y.-L. Pi, M.A. Bradford *

School of Civil and Environmental Engineering, The University of New South Wales, Sydney, NSW 2052, Australia

Received 15 March 2001; received in revised form 15 November 2001

Abstract

Arches are often connected to other members which influence the structural behaviour of the arch. These members induce restraining actions during flexural-torsional buckling which restrict the buckled shapes of the arch and may significantly influence its buckling response. This paper uses an energy method to study the elastic flexural-torsional buckling of continuously restrained arches of doubly symmetric open thin-walled cross-section in uniform bending and in uniform axial compression. Closed form solutions for the flexural-torsional buckling moment of restrained arches in uniform bending and for the flexural-torsional buckling load of restrained arches in uniform axial compression are obtained. It is found that the elastic continuous restraints are more effective in increasing the buckling resistance for arches with a large included angle than for arches with a small included angle. The first buckling mode may not correspond to the lowest buckling moment or load for arches restrained by minor axis rotational or lateral-translational restraints. It is also found that the number of half sine waves corresponding to the lowest buckling moment or load increases with the stiffness of the restraints. For restrained arches in uniform axial compression, when the restraining stiffness exceeds a limiting value, the buckling mode may change from flexural-torsional to torsional. © 2002 Published by Elsevier Science Ltd.

Keywords: Arch; Buckling; Continuous; Elastic; Flexural-torsional; Lateral-translational; Minor axis rotational; Restraint; Torsional; Warping

1. Introduction

Arches are often connected one to another by other structural members which influence in the flexural-torsional buckling action of the arch, and which may significantly influence its flexural-torsional buckling load. Roof sheeting, braces and secondary members such as purlins (Fig. 1) often have the function of increasing the buckling resistance of the arch, while fulfilling their other obvious structural roles. Such braces induce restraining actions which restrict the buckled configuration of the arch, and increase its buckling resistance. Continuous restraints are usually considered to be uniform along the length of an arch, and are often used to approximate the actions of discrete restraining members which are connected to the

* Corresponding author. Tel.: +61-2-9385-5014; fax: +61-2-9385-6139.
E-mail address: m.bradford@unsw.edu.au (M.A. Bradford).

0020-7683/02/$ - see front matter © 2002 Published by Elsevier Science Ltd.
PII: S0020-7683(02)00006-9

Nomenclature

A	cross-section area
a_n	$= L/(Rn\pi)$
b_n	$= n\pi M_{yzn}/(P_{yn}L)$
E	Young's modulus of elasticity
G	shear modulus of elasticity
I_w	warping section constant
I_x, I_y	major and minor axis second moments of area
J	torsion section constant
L	length of arch
M	applied concentrated moment about ox axis
M_{ys}	first mode flexural-torsional buckling moment of a beam in uniform bending
$M_{ys\alpha}$	first mode flexural-torsional buckling moment of a restrained beam in uniform bending
M_{ysn}	nth mode flexural-torsional buckling moment of a beam in uniform bending
M_θ	first mode flexural-torsional buckling moment of an arch in uniform bending
$M_{\theta n}$	nth mode flexural-torsional buckling moment of an arch in uniform bending
$M_{\theta n\alpha}$	nth mode flexural-torsional buckling moment of a restrained arch in uniform bending
$M_{\theta\alpha}$	first mode flexural-torsional buckling moment of a restrained arch in uniform bending
N	stress resultant (centroidal axial force)
P	an arbitrary point in cross-section
P_{sn}	nth mode torsional buckling load of a column in uniform axial compression
$P_{sn\alpha}$	nth mode torsional buckling load of a restrained column in uniform axial compression
$P_{s\theta n}$	nth mode torsional buckling load of an arch in uniform axial compression
$P_{s\theta n\alpha}$	nth mode torsional buckling load of a restrained arch in uniform axial compression
P_y	first mode flexural buckling load of a column in uniform axial compression
P_{yn}	nth mode flexural buckling load of a column in uniform axial compression
$P_{yn\alpha}$	nth mode flexural buckling load of a restrained column in uniform axial compression
$P_{y\theta n\alpha}$	nth mode flexural buckling load of a restrained arch in uniform axial compression
P_θ	first mode flexural-torsional buckling load of an arch in uniform axial compression
$P_{\theta n}$	nth mode flexural-torsional buckling load of an arch in uniform axial compression
$P_{\theta n\alpha}$	nth mode flexural-torsional buckling load of a restrained arch in uniform axial compression
$P_{\theta\alpha}$	first mode flexural-torsional buckling load of a restrained arch in uniform axial compression
q_y	radial distributed load
R	arch radius
r_0	$= \sqrt{(I_x + I_y)/A}$
t_P	distance from mid-thickness surface
u, v, w	displacements of shear centre in the ox, oy, os directions
v_0, w_0	prebuckling radial and longitudinal displacements
V	volume of member
w	axial displacement of the centroid in the os direction
x, y, s	coordinates in the ox, oy, os direction
y_r	distance of continuous minor axis rotational restraints from shear centre
y_t	distance of continuous lateral-translational restraints from shear centre
α_{rs}	stiffness of a continuous torsional restraint
α_{ry}	stiffness of a continuous minor axis rotational restraint

α_t	stiffness of a continuous lateral-translational restraint
α_w	stiffness of a continuous warping restraint
δ	first variation
δ^2	second variation
γ_P	shear strain at P
ϵ_P	longitudinal normal strain at P
Π	total potential
σ_P	longitudinal normal stress at P
τ_P	shear stress at P due to uniform torsion
ϕ	twist rotation of cross-section about the shear centre axis
Θ	arch included angle
ω	section warping function

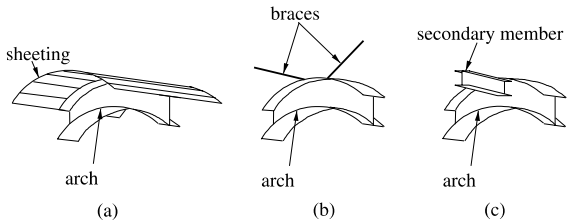

Fig. 1. Arches and out-of-plane restraint elements.

arch at closely spaced intervals. Examples of these include purlin-sheeting systems. Continuous restraints induce actions which resist the buckling deflections, rotations, twist rotations, twists and warping displacements. These restraints are usually assumed to be elastic, in which case they may be characterised by their elastic stiffnesses.

Studies of the influence of elastic restraints on the elastic flexural or torsional buckling of columns and the elastic flexural-torsional buckling of beams have been extensive. Winter (1958), Taylor and Ojalvo (1966), Nethercot (1973), Mutton and Trahair (1973), Ojalvo and Chambers (1977), Svensson and Plum (1983), Bradford (1989), Yura (1993), Trahair and Bradford (1998), Valentino and Trahair (1998) and Helwig and Yura (1999) can be cited among others. A summary of research work on the effects of elastic restraints in the elastic flexural buckling of columns and the elastic flexural-torsional buckling of beams can be found in Trahair (1993). The elastic flexural-torsional buckling of unrestrained arches has been studied by a number of researchers. Closed form solutions for arches subjected to uniformly distributed radial loads (that produce uniform axial compression) or equal and opposite end moments (that produce uniform bending) have been obtained (Timoshenko and Gere, 1961; Vlasov, 1961; Yang and Kuo, 1987; Papangelis and Trahair, 1987; Rajasekaran and Padmanabhan, 1989; Trahair, 1993; Pi et al., 1995). However, studies of the effects of elastic restraints on the elastic flexural-torsional buckling of arches do not appear to have been reported, and it is not known whether research findings relevant to the flexural-torsional buckling of restrained beams and the flexural or torsional buckling behaviour of restrained columns can be extended directly to arches. Because the flexural-torsional buckling resistance of unrestrained arches decreases with the increase of the included angle as the arch becomes deeper, it may sometimes be thought that certain arches require significant lateral bracing. However, the curved profile of an arch is quite different from that of a straight member, so that the distribution of restraining actions along the arch induced by the restraints is quite different from that along a straight member. The elastic restraints produce both restraining bending

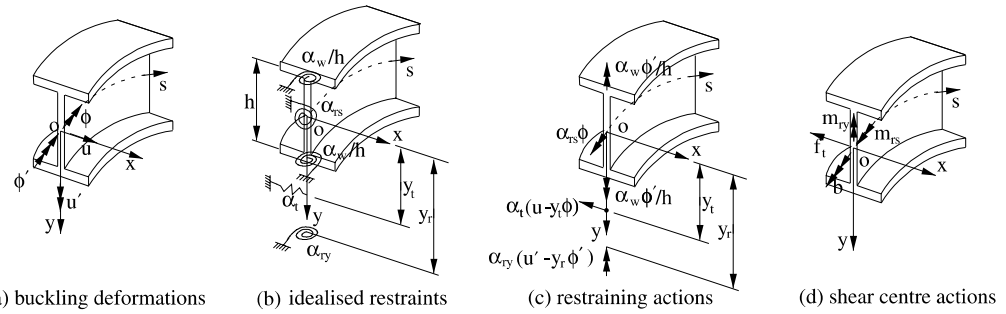

(a) buckling deformations (b) idealised restraints (c) restraining actions (d) shear centre actions

Fig. 2. Continuous restraint actions.

and torsional actions in an arch during buckling, while they produce only restraining bending actions (lateral-translational and minor axis rotational restraints) or only restraining torsional actions (torsional and warping restraints) in a straight member during buckling. Because of the different distributions of these restraining actions, lateral-translational restraints may be more efficient for arches than for beams. Therefore, research into this grey area of the out-of-plane buckling of restrained arches is much needed to fill an important gap in structural mechanics.

Arches are supported at both ends, usually in such a way that the relative end deflections away from each other are prevented, in which case the arch resists general loading by a combination of axial compression and bending actions. Before investigating the effects of elastic restraints on the flexural-torsional buckling of arches under arbitrary loading, the effects of elastic restraints on the flexural-torsional buckling of arches in uniform axial compression and in uniform bending (Fig. 2) need to be studied. The purpose of this paper is to study effects of elastic continuous restraints on the elastic flexural-torsional buckling of arches of doubly symmetric I-section in uniform bending and in uniform axial compression.

2. Total potential formulation

2.1. Elastic continuous restraints

A variable coordinate system *oxys* is introduced as shown in Fig. 2(a). The origin of the axis system coincides with the shear centre *o* of the cross-section of undeformed arch. The axes *ox* and *oy* coincide with the major and minor principal axes of the cross-section of undeformed arch. The axis *oy* also points to the centre of the undeformed arch. The axis *os* coincides with the shear centre axis of the undeformed arch.

An arch subjected to in-plane loading may suddenly buckle in a flexural-torsional mode. The vector of the buckling deformations $\{d\}$ can be defined by

$$\{d\} = \{u, u', \phi, \phi'\}^{\mathrm{T}} \tag{1}$$

where u is the displacement of the shear centre o in the direction of the axis ox, u' is the rotation about the axis oy, ϕ is the twist rotation of the cross-section about the axis os, and ϕ' is the twist per unit length about the axis os (Fig. 2(a)).

These buckling deformations may be restrained continuously by a lateral-translational restraint of stiffness α_{t} which acts at a distance y_{t} from the shear centre, by a minor axis rotational restraint of stiffness α_{ry} which acts at a distance y_{r} from the shear centre, by a torsional restraint of stiffness α_{rs}, and/or by a warping restraint of stiffness α_{w} (Fig. 2(b)). It is assumed that the restraints deform with the arch during

buckling, but remain in their original position and parallel to their original directions and planes. The actions exerted by these restraints to the arch are (Fig. 2(c)): the restraining force per unit length $\alpha_t(u - y_t\phi)$ parallel to the axis ox exerted by the lateral-translational restraint, the restraining moment per unit length $\alpha_{ry}(u' - y_t\phi')$ about an axis at y_t that is parallel to the axis oy exerted by the minor axis rotational restraint, the restraining torque per unit length $\alpha_{rs}\phi$ about the axis os exerted by the torsional restraint, and the restraining bimoment per unit length exerted by the warping restraint that is formed by the two opposite flange moments $\alpha_w\phi'/h$ where h is the distance between the flange centroids as shown in Fig. 2(b).

The shear centre actions exerted by these restraints can then be expressed as

$$\{r\} = [\alpha_b]\{d\} \tag{2}$$

where $\{r\}$ is the vector of shear centre actions given by

$$\{r\} = \{f_{rx}, m_{ry}, m_{rs}, b_{rs}\} \tag{3}$$

in which f_{rx} is the restraining force at the shear centre per unit length in the negative direction of the axis ox, m_{ry} is the restraining moment per unit length at the shear centre about the negative direction of the axis oy, m_{rs} is the restraining torque per unit length at the shear centre about the negative direction of the axis os, and b_{rs} is the bimoment per unit length at the shear centre about the negative direction of the axis os (Fig. 2(d)); and the matrix of restaining stiffnesses $[\alpha_b]$ is given by

$$[\alpha_b] = \begin{bmatrix} \alpha_t & 0 & -\alpha_t y_t & 0 \\ 0 & \alpha_{ry} & 0 & -\alpha_{ry} y_r \\ -\alpha_t y_t & 0 & \alpha_t y_t^2 + \alpha_{rs} & 0 \\ 0 & -\alpha_{ry} y_r & 0 & \alpha_{ry} y_r^2 + \alpha_w \end{bmatrix} \tag{4}$$

It is noted that the restraining force f_{rx} and the restraining moment m_{ry} induce both bending and torsional restraining actions in an arch during buckling, while they induce only a bending restraining action in a straight member during buckling. The restraining torque m_{rs} induces both torsional and bending restraining actions in an arch during buckling, while it induces only a torsional restraining action in a straight member during buckling.

2.2. Total potential

The total potential of a restrained arch in uniform bending and uniform compression actions can be written as

$$\Pi = \int_V \{\epsilon_P \ \gamma_P\}\{\sigma_P \ \tau_P\}^T \mathrm{d}v + \int_0^L \{r\}^T\{d\}\mathrm{d}s - \int_0^L q_y v \,\mathrm{d}s + \sum \{R\}^T\{D\} - \sum_{0,L}(-M_x v') \tag{5}$$

where ϵ_P is the longitudinal normal strain at a point P on the cross-section that satisfies the Vlasov assumptions (Vlasov, 1961) given by (Pi et al., 1995; Pi and Bradford, 2001)

$$\begin{aligned} \epsilon_P = {} & \left(w' - \frac{v}{R}\right) + \frac{1}{2}u'^2 + \frac{1}{2}\left(v' + \frac{w}{R}\right)^2 - x\left[u''\cos\phi + \left(v'' + \frac{w'}{R}\right)\sin\phi + \frac{\sin\phi}{R}\right] \\ & + y\left[u''\sin\phi - \left(v'' + \frac{w'}{R}\right)\cos\phi - \frac{\cos\phi}{R} + \frac{1}{R}\right] - \omega\left(\phi'' - \frac{u''}{R}\right) + \frac{1}{2}(x^2 + y^2)\left(\phi' - \frac{u'}{R}\right)^2 \end{aligned} \tag{6}$$

in which x, y are the coordinates of the point P in the principal axes oxy as shown in Fig. 3(a), ω is the section warping function; γ_P is the shear strain at a point P on the cross-section due to uniform torsion and given by (Vlasov, 1961; Pi et al., 1995; Pi and Bradford, 2001)

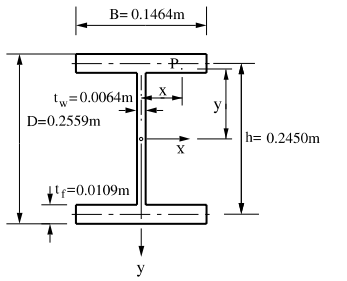

Fig. 3. Arch cross-section and properties.

$$\gamma_P = \begin{cases} -2(y+\frac{h}{2})(\phi' - \frac{u'}{R}) & \text{for the top flange} \\ 2x(\phi' - \frac{u'}{R}) & \text{for the web} \\ -2(y-\frac{h}{2})(\phi' - \frac{u'}{R}) & \text{for the bottom flange} \end{cases} \tag{7}$$

and σ_P and τ_P are the longitudinal normal and uniform torsional shear stresses given by

$$\sigma_P = E\epsilon_P \quad \text{and} \quad \tau_P = G\gamma_P \tag{8}$$

in which E is the Young's modulus of elasticity and G is the shear modulus of elasticity.

3. Energy equation

Because it can accurately predict the flexural-torsional buckling of an arch (Pi et al., 1995), the classical buckling theory is used herein to establish the critical condition for the buckling. In the classical theory, the critical condition for buckling is that the second variation $\frac{1}{2}\delta^2\Pi$ of the total potential Π given by (5) vanishes for any arbitrary variation of the displacement field. This buckling criterion is often called the energy equation which can be stated in a standard variational form as

$$\frac{1}{2}\delta^2\Pi = \int_0^L F(s,u,u',u'',\phi,\phi',\phi'')\mathrm{d}s = 0 \tag{9}$$

and from (5)

$$F(s,u,u',u'',\phi,\phi',\phi'') = \frac{1}{2}\left\{\left[EI_y\left(u'' + \frac{\phi}{R}\right)^2 + EI_w\left(\phi'' - \frac{u''}{R}\right)^2 + GJ\left(\phi' - \frac{u'}{R}\right)\right] + N\left[(u')^2 + r_0^2\left(\phi' - \frac{u'}{R}\right)^2\right] + M\left[2u''\phi + \frac{\phi^2}{R}\right] + \{d\}^{\mathrm{T}}[\alpha_b]\{d\}\right\} \tag{10}$$

where the variation signs δ for the variation of the lateral buckling displacement δu and the buckling twist rotation $\delta\phi$ have been dropped for simplicity, L is the length of the arch, I_y is the second moment of the area of the cross-section about the minor axis oy, I_w is the warping constant of the cross-section; J is the torsion constant of the cross-section; r_0 is the polar gyration radius of the cross-section defined by

$$r_0 = \sqrt{\frac{I_x + I_y}{A}} \tag{11}$$

in which A is the area of the cross-section and I_x is the second moment of the area of the cross-section about its major axis; and N and M are the prebuckling stress resultants given by

$$N = \int_A \sigma_{P0}\,\mathrm{d}A = EA(w_0' - v_0/R) \tag{12}$$

and

$$M = \int_A \sigma_{P0} y\,\mathrm{d}A = EI_x(v_0'' + w_0'/R) \tag{13}$$

in which v_0 and w_0 are the prebuckling radial and axial displacements respectively.

The differential equilibrium equations for the flexural-torsional buckling of an arch can be obtained from the energy equation (9) by invoking the calculus of variations, according to which the functions u and ϕ which make the functional

$$\frac{1}{2}\delta^2 \Pi = \int_0^L F(s, u, u', u'', \phi, \phi', \phi'')\mathrm{d}s \tag{14}$$

stationary satisfy the Euler–Lagrange equations

$$\frac{\partial F}{\partial u} - \frac{\mathrm{d}}{\mathrm{d}s}\left(\frac{\partial F}{\partial u'}\right) + \frac{\mathrm{d}^2}{\mathrm{d}s^2}\left(\frac{\partial F}{\partial u''}\right) = 0 \tag{15}$$

and

$$\frac{\partial F}{\partial \phi} - \frac{\mathrm{d}}{\mathrm{d}s}\left(\frac{\partial F}{\partial \phi'}\right) + \frac{\mathrm{d}^2}{\mathrm{d}s^2}\left(\frac{\partial F}{\partial \phi''}\right) = 0 \tag{16}$$

which leads to

$$\begin{aligned}&[EI_y(u'' + \phi/R)]'' - [EI_{\mathrm{w}}(\phi'' - u''/R)/R]'' + [GJ(\phi' - u'/R)/R]' + \alpha_{\mathrm{t}} u - \alpha_{\mathrm{t}} y_{\mathrm{t}}\phi - (\alpha_{\mathrm{r}y}u')'\\ &\quad + (\alpha_{\mathrm{r}y} y_{\mathrm{r}}\phi')' - (Nu')' + [N(\phi' - u'/R)(r_0^2/R)]' + (M\phi)'' = 0\end{aligned} \tag{17}$$

for bending about the minor axis oy, and to

$$\begin{aligned}&EI_y(u'' + \phi/R)/R + [EI_{\mathrm{w}}(\phi'' - u''/R)]'' - [GJ(\phi' - u'/R)]' + (\alpha_{\mathrm{rs}} + \alpha_{\mathrm{t}} y_{\mathrm{t}}^2)\phi - [(\alpha_{\mathrm{w}} + \alpha_{\mathrm{r}y} y_{\mathrm{r}}^2)\phi']'\\ &\quad - \alpha_{\mathrm{t}} y_{\mathrm{t}} u + (\alpha_{\mathrm{r}y} y_{\mathrm{r}} u')' - [Nr_0^2(\phi' - u'/R)]' + Mu'' + M\phi/R = 0\end{aligned} \tag{18}$$

for torsion about the shear axis os.

4. Arches in uniform bending

4.1. Flexural-torsional buckling

As shown in Fig. 4(a), when a continuously restrained arch that is simply supported in-plane (the boundary conditions are $v_A = v_B = w_A = 0$) and out-of-plane (the boundary conditions are $u_A = u_B = \phi_A = \phi_B$) is subjected to equal and opposite end moments M_x about the axes ox through the both ends of undeformed arch, the arch is primarily under uniform bending action and its horizontal reactions are equal to zero. It is assumed that the end moments M_x remain in the initial acting positions during deformation and do not move with ends of the arch. The restrained arch in uniform bending may suddenly buckle under a constant buckling moment M_x and the possible buckled configuration can be approximated by

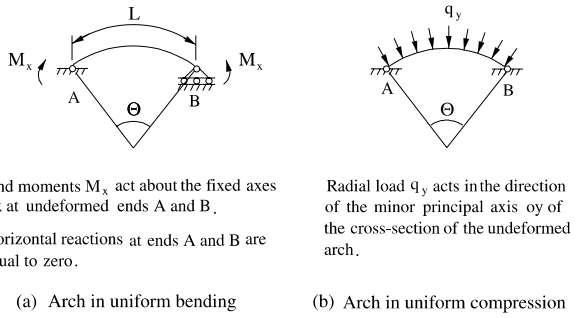

Fig. 4. Arches in uniform bending and uniform compression.

$$\frac{u}{\delta}=\frac{\phi}{\varphi}=\sin\frac{n\pi s}{L} \tag{19}$$

where δ and φ are the maximum values of u and ϕ and n is the number of buckled half waves around the arch axis.

Substituting (19) into (17) and (18) leads to

$$\frac{1}{2}\frac{L}{2}\frac{n^2\pi^2}{L^2}\begin{Bmatrix}\delta\\ \varphi\end{Bmatrix}^{\mathrm{T}}\begin{bmatrix}k_{11} & k_{12}\\ k_{21} & k_{22}\end{bmatrix}\begin{Bmatrix}\delta\\ \varphi\end{Bmatrix}=0 \tag{20}$$

where

$$k_{11}=\left[1+a_n^2b_n^2+\frac{\alpha_{\mathrm{t}}(L/n\pi)^2+\alpha_{\mathrm{ry}}}{P_{yn}}\right]P_{yn} \tag{21}$$

$$k_{12}=k_{21}=-\left[\frac{a_n}{b_n}+a_nb_n+\frac{\alpha_{\mathrm{r}y}y_{\mathrm{r}}+\alpha_{\mathrm{t}}y_{\mathrm{t}}(L/n\pi)^2}{M_{ysn}}+\frac{M}{M_{ysn}}\right]M_{ysn} \tag{22}$$

$$k_{22}=\left[1+\frac{a_n^2}{b_n^2}+\frac{(\alpha_{\mathrm{rs}}+\alpha_{\mathrm{t}}y_{\mathrm{t}}^2)(L/n\pi)^2}{r_0^2P_{sn}}+\frac{(\alpha_{\mathrm{w}}+\alpha_{\mathrm{r}y}y_{\mathrm{r}}^2)}{r_0^2P_{sn}}+\frac{a_n}{b_n}\frac{M}{M_{ysn}}\right]r_0^2P_{sn} \tag{23}$$

The dimensionless parameters a_n and b_n in (21)–(23) are defined as

$$a_n=\frac{L}{n\pi R} \tag{24}$$

$$b_n=\frac{n\pi M_{ysn}}{P_{yn}L} \tag{25}$$

where P_{yn} is the nth mode minor axis flexural buckling load of a column in uniform axial compression given by

$$P_{yn}=\frac{n^2\pi^2EI_y}{L^2} \tag{26}$$

and M_{ysn} is the nth mode flexural-torsional buckling moment of a beam in uniform bending given by

$$M_{ysn}=\sqrt{r_0^2P_{yn}P_{sn}} \tag{27}$$

in which P_{sn} is the nth mode torsional buckling load of a column in uniform axial compression given by

$$P_{sn} = \frac{1}{r_0^2}\left(GJ + \frac{n^2\pi^2 EI_w}{L^2}\right) \tag{28}$$

The condition for a nontrivial solution of δ and φ from Eq. (20) is

$$k_{12}k_{21} = k_{11}k_{22} \tag{29}$$

which leads to the buckling moment of an unrestrained arch ($\alpha_{rs} = \alpha_w = \alpha_{ry} = \alpha_t = 0$) in uniform bending (Vlasov, 1961; Papangelis and Trahair, 1987; Pi et al., 1995)

$$M_{\theta n} = k_{\theta n} M_{ysn} \tag{30}$$

where $k_{\theta n}$ is the buckling factor for an unrestrained arch in uniform bending given by

$$k_{\theta n} = -a_n b_n - \frac{a_n}{2b_n} + \frac{a_n^3 b_n}{2} + \sqrt{\left(a_n b_n + \frac{a_n}{2b_n} - \frac{a_n^3 b_n}{2}\right)^2 + (1 - a_n^2)^2} \tag{31}$$

The lowest buckling moment M_θ of an unrestrained arch in uniform bending corresponds to a single half sine wave buckled shape ($n = 1$).

When the elastic restraints are considered, however, a number of trials generally need to be made before the integer value of n which leads to the lowest buckling moment $M_{\theta n}$ can be determined.

4.2. Torsional buckling

When the lateral displacements u and minor axis rotations u' at the shear centre axis of a restrained arch are fully prevented ($u = u' = 0$), the arch may buckle torsionally and the differential equilibrium equation for torsional buckling can be obtained from (18) as

$$EI_y\phi/R^2 + (EI_w\phi'')'' - (GJ\phi')' + \alpha_{rs}\phi - (\alpha_w\phi')' + M\phi/R = 0 \tag{32}$$

The torsional buckling moment of the arch can be obtained from (32) by assuming $\phi = \varphi \sin(n\pi s/L)$ as

$$\frac{M_{\theta n}}{M_{ysn}} = -\left(\frac{a_n}{b_n} + \frac{b_n}{a_n}\right) \tag{33}$$

4.3. Effects of torsional and warping restraints

The lowest flexural-torsional buckling moment for an arch in uniform bending restrained by continuous torsional and warping restraints corresponds to a single half sine wave ($n = 1$), and can be obtained from (29) as

$$M_{\theta\alpha} = k_{\theta\alpha} M_{ys} \tag{34}$$

where $k_{\theta\alpha}$ is the buckling factor for a restrained arch in uniform bending given by

$$k_{\theta\alpha} = -a_1 b_1 - \frac{a_1}{2b_1} + \frac{a_1^3 b_1}{2} + \sqrt{\left(a_1 b_1 + \frac{a_1}{2b_1} - \frac{a_1^3 b_1}{2}\right)^2 + (1 - a_1^2)^2 + (1 + a_1^2 b_1^2)\left(\frac{\alpha_{rs}(L/\pi)^2 + \alpha_w}{r_0^2 P_s}\right)} \tag{35}$$

in which the parameters a_1 and b_1 are given by (24) and (25) with $n = 1$ and P_s is the first mode torsional buckling load of the corresponding column given by (28) with $n = 1$, and M_{ys} is the first mode flexural-torsional buckling moment of the corresponding beam in uniform bending given by (27) with $n = 1$.

The buckling moment given by (34) neglects the effects of prebuckling in-plane deflections which reduce the radius of the arch and increase the buckling moment. An approximate increased buckling moment including the effects of prebuckling in-plane deflections can be expressed in a similar way as that for an unrestrained arch (Pi et al., 1995) and given by

$$M_{\theta\alpha d} = \frac{M_{\theta\alpha}}{\sqrt{(1 - I_y/I_x)(1 - (GJ + \pi^2 EI_w/L^2)/2EI_x)}} \tag{36}$$

The universal section 250UB37 shown in Fig. 3, with Young's modulus of elasticity $E = 200{,}000$ MPa and shear modulus of elasticity $G = 80{,}000$ MPa has been used (and also used later in this paper) to calculate the buckling moment of restrained arches. To show further that the classical buckling theory can accurately predict the flexural-torsional buckling resistance of restrained arches, the buckling moments given by (34) and (36) are compared with results of a nonlinear finite element analysis (Pi and Trahair, 1996) in Fig. 5. Because the nonlinear finite element analysis includes the effects of the prebuckling in-plane deflections, the buckling moment predicted by finite element results are slightly higher than those predicted by Eq. (34) and agree very well with those predicted by Eq. (36).

Variations of the dimensionless buckling moment $M_{\theta\alpha}/M_{ys}$ with the included angle Θ obtained from (34) are shown in Fig. 6 for arches with different dimensionless restraining stiffness α_{rs}/P_y. It can be seen that the buckling moment of an unrestrained arch in uniform bending ($\alpha_{rs}/P_y = 0$) decreases from $M_{\theta\alpha}/M_{ys} = 1$ to $M_{\theta\alpha}/M_{ys} = 0$ as the included angle increases from $\Theta = 0°$ to $\Theta = 180°$. It can be observed in Fig. 6 that torsional restraints increase the buckling moment of an arch, and are more effective for arches with a larger included angle than for arches with a smaller included angle.

4.4. Effects of minor axis rotational restraints

The lowest flexural-torsional buckling moment of a beam in uniform bending restrained by continuous minor axis rotational restraints corresponds to a single half sine wave (Trahair, 1993). However, an arch restrained by continuous minor axis rotational restraints may buckle in more than one half sine waves, and the equation for the buckling moment can be obtained from (29) as

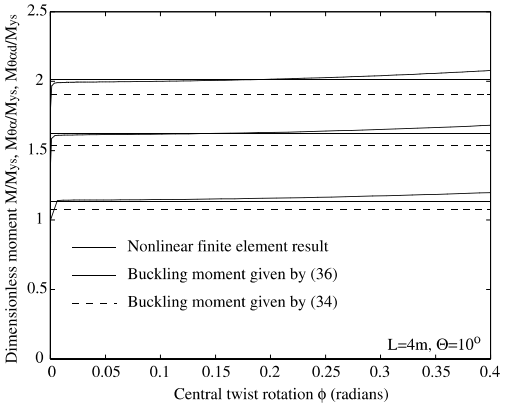

Fig. 5. Comparison with nonlinear analysis results.

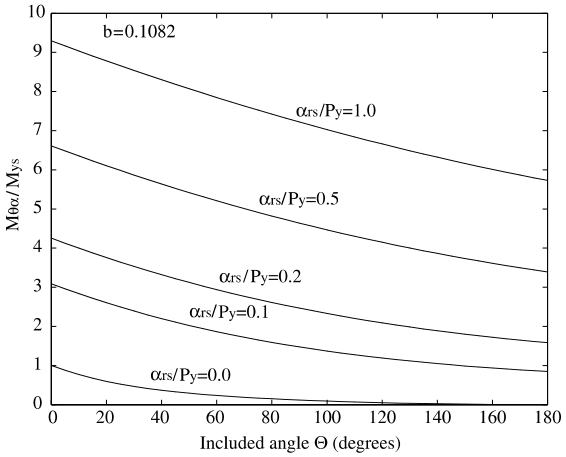

Fig. 6. Flexural-torsional buckling moment for arches in uniform bending with continuous torsional restraints.

$$A_1\left(\frac{M_{\theta n\alpha}}{M_{ysn}}\right)^2 + B_1\left(\frac{M_{\theta n\alpha}}{M_{ysn}}\right) + C_1 = 0 \tag{37}$$

where

$$A_1 = 1 \tag{38}$$

$$B_1 = 2a_n b_n + \frac{a_n}{b_n} - a_n^3 b_n + \frac{\alpha_{ry}}{n^2 P_y}\left(\frac{2y_r P_{yn}}{M_{ysn}} - \frac{a_n}{b_n}\right) \tag{39}$$

$$C_1 = -(1-a_n^2)^2 - \frac{\alpha_{ry}}{n^2 P_y}\left[\left(1-\frac{y_r}{R}\right)^2 + \left(\frac{y_r P_{yn}}{M_{ysn}} - \frac{a_n}{b_n}\right)^2\right] \tag{40}$$

The lowest buckling moment $M_{\theta n\alpha}$ for given restraining stiffness α_{ry} acting at y_t may be determined by calculating successive values of $M_{\theta n\alpha}/M_{ys}$ with the number of half waves $n = 1, 2, 3, \ldots$ Fig. 7 shows a

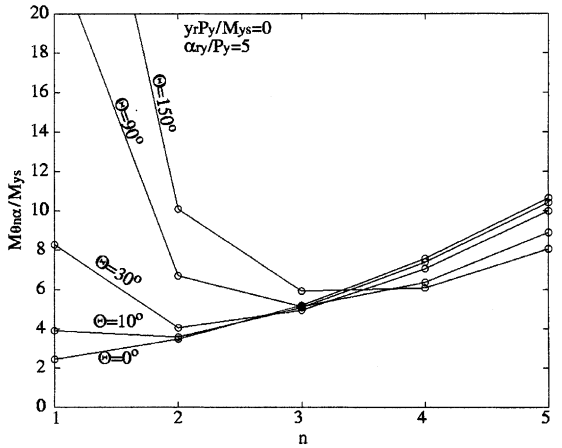

Fig. 7. Buckling mode for arches in uniform bending with continuous minor axis rotational restraints.

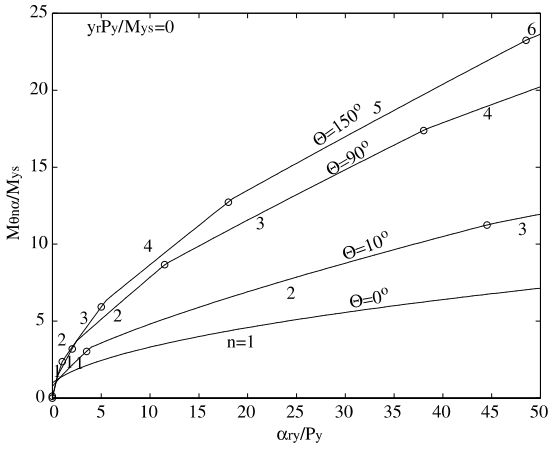

Fig. 8. Flexural-torsional buckling of arches in uniform bending with continuous minor axis rotational restraints.

typical case of the relationship of the dimensionless buckling moment $M_{\theta n\alpha}/M_{ys}$ with the number of half waves when $\alpha_{ry}/P_y = 5$ and $y_t P_y/M_{ys} = 0$. In general, these moments will decrease at first until the minimum is reached, and will then increase. Thus the successive calculation may be terminated when there is an increase in $M_{\theta n\alpha}/M_{ys}$.

Variations of the dimensionless buckling moment $M_{\theta n\alpha}/M_{ys}$ with the dimensionless restraining stiffness α_{ry}/P_y obtained from (37) are shown in Fig. 8 for arches with different included angles Θ. It can be seen that the number of half sine waves n corresponding to the lowest buckling moment increases with the increase of the restraining stiffness α_{ry}/P_y and the included angle Θ. For example, for the restraining stiffness $\alpha_{ry}/P_y = 15$, the beam ($\Theta = 0°$) buckles in a single half sine wave, the arch with an included angle $\Theta = 10°$ buckles in two half sine waves while the arch with an included angle $\Theta = 90°$ buckles in three half sine waves, while the arch with an included angle $\Theta = 150°$ buckles in four half sine waves. It can also be seen in Fig. 8 that continuous minor axis rotational restraints are much more effective for arches with a larger included angle than for arches with a smaller included angle. For example, the buckling moment of an unrestrained arch with an included angle $\Theta = 90°$ ($M_\theta/M_{ys} \approx 0.12$) is lower than that of an unrestrained arch with an included angle $\Theta = 10°$ ($M_\theta/M_{ys} \approx 0.77$). However, when the arch is restrained by a continuous minor axis rotational restraint of dimensionless stiffness $\alpha_{ry}/P_y = 10$, the buckling moment of the arch with $\Theta = 90°$ ($M_{\theta n\alpha}/M_{ys} = 7.99$) is higher than that of the arch with $\Theta = 10°$ ($M_{\theta n\alpha}/M_{ys} = 4.75$).

When the value of the restraining stiffness α_{ry} approaches infinity, the limiting value of the dimensionless buckling moment is

$$\lim_{\alpha_{ry}/P_y \to \infty} \left(\frac{M_{\theta n\alpha}}{M_{ysn}} \right) = \frac{(1 - a_n b_n (y_r P_{yn}/M_{ysn}))^2 + ((y_r P_{yn}/M_{ysn}) - (a_n/b_n))^2}{2((y_r P_{ym}/M_{ysn}) - (a_n/2b_n))} \tag{41}$$

which corresponds to the case where the arch buckles with an enforced centre of rotation. When the enforced centre of rotation is the shear centre of the cross-section, the limiting value (41) ($y_r = 0$) is equal to the torsional buckling moment of an arch given by (33).

The limiting value (41) can be reduced to the following limiting value of the first mode buckling moment for a beam when the included angle $\Theta = 0°$ (i.e. $n = 1$ and $a_1 = 0$) given by Trahair (1993)

$$\lim_{\alpha_{ry}/P_y \to \infty} \left(\frac{M_{ys\alpha}}{M_{ys}} \right) = \frac{1}{2} \left(\frac{y_r P_y}{M_{ys}} + \frac{M_{ys}}{y_r P_y} \right) \tag{42}$$

It is of interest to note that when the minor axis rotations of an arch are fully prevented ($u' = 0$) at the arch shear centre axis ($y_r = 0$ and $\alpha_{ry} = \infty$), the arch will buckle torsionally at the moment

$$\frac{M_{\theta n\infty}}{M_{ysn}} = -\left(\frac{b_n}{a_n} + \frac{a_n}{b_n}\right) \tag{43}$$

which is consistent with the torsional buckling moment of an unrestrained arch given by (33). However, for a beam, when minor axis rotations are fully prevented ($u' = 0$) at $y_r = 0$, the beam does not buckle because $\lim_{\Theta\to 0} M_{ys\theta\infty}/M_{ys} = \infty$.

It can be observed further from (41) that if the minor axis rotations of an arch are fully restrained at $y_r = a_n M_{ysn}/2b_n P_{yn}$ i.e. $y_r = M_{ysn}a_n/(2P_{yn}b_n) = L\Theta/(2n^2\pi^2)$, the arch does not buckle because $\lim_{y_r\to L\Theta/(2n^2\pi^2)} M_{\theta n\infty}/M_{ysn} = \infty$.

Variations of the dimensionless buckling moment $M_{\theta n\alpha}/M_{ys}$ with the dimensionless restraint height $y_r P_y/M_{ys}$ obtained from (37) are shown in Fig. 9 for arches (included angle $\Theta = 10°$) with different values of the dimensionless restraining stiffness α_{ry}/P_y. In general, the buckling moment $M_{\theta n\alpha}/M_{ys}$ increases with an increase in the restraining stiffness α_{ry}/P_y. When the restraint acts above the shear centre ($y_r P_y/M_{ys} < 0$), the dimensionless buckling moment $M_{\theta n\alpha}/M_{ys}$ increases indefinitely with the restraining stiffness α_{ry}. Restraints acting below the shear centre ($y_r P_y/M_{ys} > 0$) are comparatively ineffective. It can also be seen that the number of half sine waves n corresponding to the lowest buckling moment increases with a decrease in the restraint height from $y_r P_y/M_{ys} = 2$ (below the shear centre) to $y_r P_y/M_{ys} = -2$ (above the shear centre).

Variations of the dimensionless buckling moment $M_{\theta n\alpha}/M_{ys}$ with the dimensionless restraining stiffness α_{ry}/P_y obtained from (37) are shown in Fig. 10 for arches (included angle $\Theta = 10°$ and dimensionless restraint height $y_t P_y/M_{ys} = 0$) with different values of the torsional parameter K defined by

$$K = \sqrt{\frac{\pi^2 EI_w}{GJL^2}} \tag{44}$$

It can be seen that the number of half sine waves n corresponding to the lowest buckling moment increases as the torsional parameter K decreases.

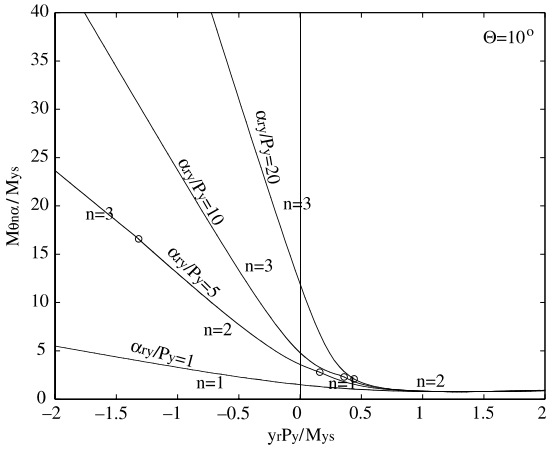

Fig. 9. Effects of restraint height on buckling of arches in uniform bending with continuous minor axis rotational restraints.

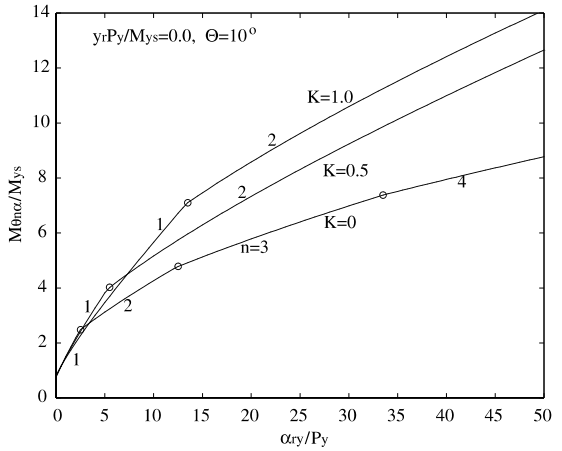

Fig. 10. Effects of torsional parameter on buckling of arches in uniform bending with continuous minor axis rotational restraints.

4.5. Effects of lateral-translational restraints

Arches restrained by continuous lateral-translational restraints may buckle in n half sine waves, and the equation for the flexural-torsional buckling moment can be obtained from (29) as

$$A_2\left(\frac{M_{\theta n\alpha}}{M_{ysn}}\right)^2 + B_2\left(\frac{M_{\theta n\alpha}}{M_{ysn}}\right) + C_2 = 0 \tag{45}$$

where

$$A_2 = 1 \tag{46}$$

$$B_2 = 2a_n b_n + \frac{a_n}{b_n} - a_n^3 b_n + \frac{\alpha_t (L/\pi)^2}{n^4 P_y}\left(\frac{2y_t P_{yn}}{M_{ysn}} - \frac{a_n}{b_n}\right) \tag{47}$$

$$C_2 = -(1-a_n^2)^2 - \frac{\alpha_t (L/\pi)^2}{n^4 P_y}\left[\left(1-\frac{y_t}{R}\right)^2 + \left(\frac{y_t P_{yn}}{M_{ysn}} - \frac{a_n}{b_n}\right)^2\right] \tag{48}$$

The lowest buckling moment $M_{\theta n\alpha}$ for given restraining stiffness α_t acting at height y_t may be determined in the same way as for arches restrained by continuous minor axis rotational restraints as discussed above.

Variations of the dimensionless buckling moment $M_{\theta n\alpha}/M_\theta$ with the dimensionless restraining stiffness $\alpha_t(L/\pi)^2/P_y$ obtained from (45) are shown in Fig. 11 for arches with different included angle Θ. It can be seen that the number n of half sine waves corresponding to the lowest buckling moment increases with the increase of the restraining stiffness $\alpha_t(L/\pi)^2/P_y$ and the included angle Θ. For example, when $\alpha_t(L/\pi)^2/P_y = 15$, the number of half sine waves $n = 2$ for the beam ($\Theta = 0°$) and arches with included angles $\Theta = 10°$ and 30°, and $n = 3$ for the arch with $\Theta = 60°$. Continuous lateral-translational restraints are much more effective for arches with a larger included angle than for arches with a smaller included angle.

Variations of the dimensionless buckling moment $M_{\theta n\alpha}/M_{ys}$ with the dimensionless restraint height $y_t P_y/M_{ys}$ obtained from (45) are shown in Fig. 12 for arches (included angle $\Theta = 10°$) with different values

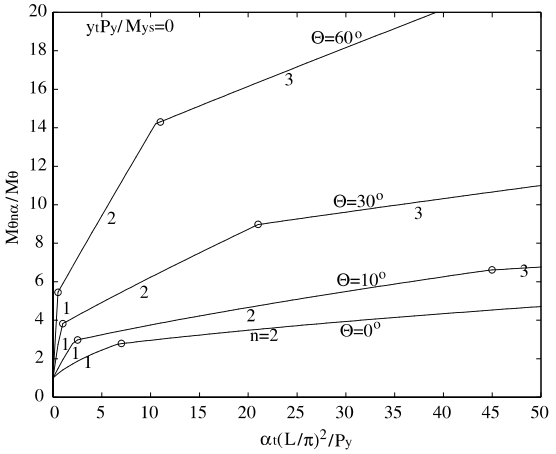

Fig. 11. Flexural-torsional buckling of arches in uniform bending with continuous lateral-translational restraints.

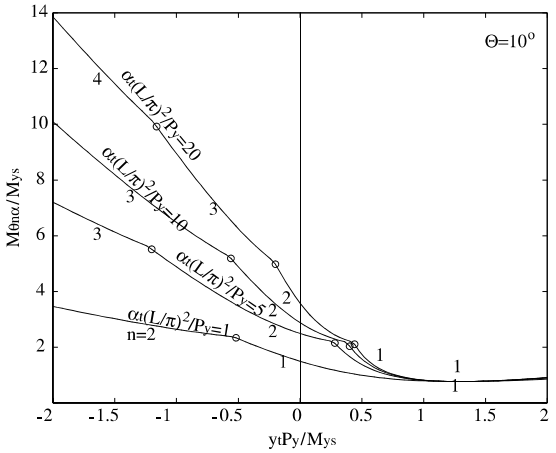

Fig. 12. Effect of restraint height on buckling of arches in uniform bending with continuous lateral-translational restraints.

of the dimensionless restraining stiffness $\alpha_t(L/\pi)^2/P_y$. In general, the buckling moment $M_{\theta n\alpha}/M_{ys}$ increases with an increase in the restraining stiffness $\alpha_t(L/\pi)^2/P_y$. When the restraint acts above the shear centre ($y_tP_y/M_{ys} < 0$), the buckling moment $M_{\theta n\alpha}/M_{ys}$ increases indefinitely with the increase of the restraining stiffness $\alpha_t(L/\pi)^2/P_y$. Restraints acting below the shear centre ($y_tP_y/M_{ys} > 0$) are comparatively ineffective. The number of half sine waves n corresponding to the lowest buckling moment increases whenthe restraint position y_tP_y/M_{ys} moves from below the shear centre ($y_t > 0$) to above the shear centre ($y_t < 0$).

Variations of the dimensionless buckling moment $M_{\theta n\alpha}/M_{ys}$ with the dimensionless restraining stiffness $\alpha_t(L/\pi)^2P_y$ obtained from (45) are shown in Fig. 13 for arches (included angle $\Theta = 10°$ and dimensionless restraint height $y_tP_y/M_{ys} = 0$) with different values of the torsional parameter K. It can be seen that the number of half sine waves n during buckling increases as the torsional parameter K decreases.

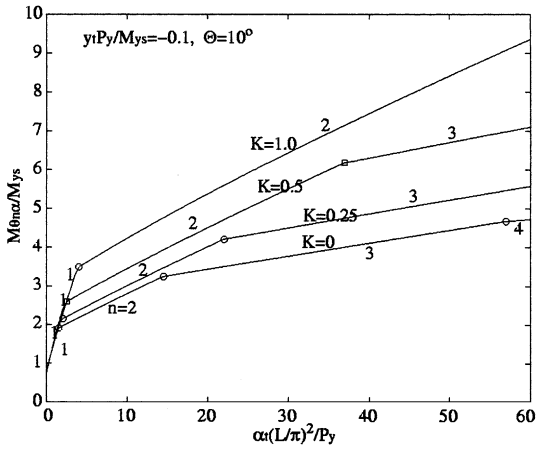

Fig. 13. Effect of torsional parameter on buckling of arches in uniform bending with continuous lateral-translational restraints.

5. Arches in uniform axial compression

5.1. Flexural-torsional buckling

As shown in Fig. 4(b), when an arch that is pin-ended in-plane (the boundary conditions are $v_A = v_B = w_A = w_B = 0$) and simply supported out-of-plane (the boundary conditions are $u_A = u_B = \phi_A = \phi_B$) is subjected to a radial load q_y uniformly distributed around the arch axis that acts in the direction of the minor principal axis of the cross-section of the undeformed arch and towards the centre of the undeformed arch and remains in the initial acting position during deformation, the arch is primarily under uniform axial compression action $P = q_y R$ which is related to the axial stress resultant N as $P = -N$. An arch in uniform compression restrained by continuous elastic restraints may buckle in a flexural-torsional mode and its possible buckled shapes can be approximated by

$$\frac{u}{\delta} = \frac{\phi}{\varphi} = \sin\frac{n\pi s}{L} \tag{49}$$

which corresponds to n buckled half sine waves around the length L of the arch.

Substituting (49) into (17) and (18) leads to

$$\frac{1}{2}\frac{n^2\pi^2}{L^2}\begin{Bmatrix}\delta\\ \varphi\end{Bmatrix}^{\mathrm{T}}\begin{bmatrix}k_{11} & k_{12}\\ k_{21} & k_{22}\end{bmatrix}\begin{Bmatrix}\delta\\ \varphi\end{Bmatrix} = 0 \tag{50}$$

where

$$k_{11} = \left[1 + a_n^2 b_n^2 + \frac{\alpha_{\mathrm{t}}(L/n\pi)^2 + \alpha_{\mathrm{ry}}}{P_{yn}} - \left(1 + \frac{r_0^2}{R^2}\right)\frac{P}{P_{yn}}\right]P_{yn} \tag{51}$$

$$k_{12} = k_{21} = -\left[\frac{a_n}{b_n} + a_n b_n + \frac{\alpha_{\mathrm{ry}} y_{\mathrm{r}} + \alpha_{\mathrm{t}} y_{\mathrm{t}}(L/n\pi)^2}{M_{ysn}} - \frac{r_0^2}{R}\frac{P_{yn}}{M_{ysn}}\frac{P}{P_{yn}}\right]M_{ysn} \tag{52}$$

$$k_{22}=\left[1+\frac{a_n^2}{b_n^2}+\frac{(\alpha_{\mathrm{rs}}+\alpha_{\mathrm{t}}y_{\mathrm{t}}^2)(L/n\pi)^2}{r_0^2P_{sn}}+\frac{(\alpha_{\mathrm{w}}+\alpha_{\mathrm{r}y}y_{\mathrm{r}}^2)}{r_0^2P_{sn}}-\frac{P_{yn}}{P_{sn}}\frac{P}{P_{yn}}\right]r_0^2P_{sn} \tag{53}$$

Eq. (50) has nontrivial solutions for δ and φ when

$$k_{12}k_{21}=k_{11}k_{22} \tag{54}$$

which leads to the flexural-torsional buckling load of an unrestrained arch in uniform compression

$$P_{\theta n}=k_{\theta n}P_{yn} \tag{55}$$

where $k_{\theta n}$ is the buckling factor of an unrestrained arch in uniform compression given by

$$k_{\theta n}=\frac{1}{2}\frac{P_{sn}}{P_{yn}}\left[\sqrt{\left(1+\frac{a_n^2}{b_n^2}\right)^2+2\left(\frac{a_n^2}{b_n^2}-1\right)(1-a_n^2)^2\frac{P_{yn}}{P_{sn}}+(1-a_n^2)^4\frac{P_{yn}^2}{P_{sn}^2}}-\left(1+\frac{a_n^2}{b_n^2}\right)-(1-a_n^2)^2\frac{P_{yn}}{P_{sn}}\right] \tag{56}$$

and P_{yn} and P_{sn} are given by (26) and (28), respectively.

The lowest buckling load P_{theta} of an unrestrained arch corresponds to a single sine wave buckled shape and is given by (55) with $n=1$. The lowest buckling load P_{theta} decreases from P_y to zero as the included angle increases from $\Theta=0^\circ$ to 180° as shown in Fig. 14(a).

It is worth pointing out that the uniformly distributed radial load q_y is different from one that stays normal to the deformed arch such as hydrostatic pressure.

5.2. Flexural buckling

When the twist rotations of the cross-section are fully prevented ($\phi=\phi'=\phi''=0$), a restrained arch in uniform compression may buckle in a flexural mode. The differential equilibrium equation for flexural buckling of an arch can be obtained from (17) as

$$(EI_yu'')''+(EI_{\mathrm{w}}u''/R^2)''-(GJu'/R^2)'+\alpha_{\mathrm{t}}u-(\alpha_{\mathrm{r}y}u')'-(Nu')'-(Nu'r_0^2/R^2)'=0 \tag{57}$$

Substituting $u=\delta\sin(n\pi s/L)$ into (57) leads to the flexural buckling load of a restrained arch in uniform axial compression given by

$$P_{y\theta n\alpha}=-N=\frac{1}{1+r_0^2/R^2}\left[\frac{(n\pi)^2EI_y}{L^2}+\left(GJ+\frac{(n\pi)^2EI_{\mathrm{w}}}{L^2}\right)\frac{1}{R^2}+\frac{\alpha_{\mathrm{t}}L^2}{(n\pi)^2}+\alpha_{\mathrm{r}y}\right] \tag{58}$$

which can be reduced to the flexural buckling load of a doubly symmetric column about its minor principal axis given by (Trahair, 1993)

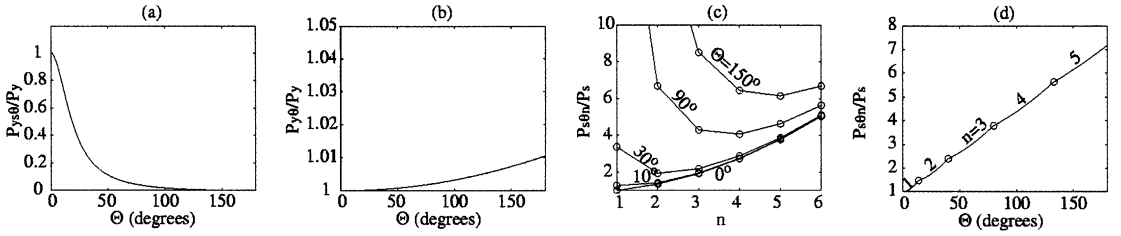

Fig. 14. Buckling of arches in uniform compression.

$$P_{yn\alpha} = n^2 P_y + \frac{\alpha_t L^2}{(n\pi)^2} + \alpha_{ry} \tag{59}$$

The lowest flexural buckling load $P_{y\theta}$ of an arch corresponds to a single half sine wave buckled shape and is given by (58) with $n = 1$ and $\alpha_t = \alpha_{ry} = 0$. The lowest flexural buckling load $P_{y\theta}$ increases slightly with the increase of the included angle Θ as shown in Fig. 14(b).

5.3. Torsional buckling

When the lateral deformations of a restrained arch in uniform compression are fully prevented ($u = u' = u'' = 0$), it may buckle in a torsional mode. The differential equilibrium equation for the torsional buckling of a restrained arch can be obtained from (18) as

$$EI_y\phi/R^2 + (EI_w\phi'')'' - (GJ\phi')' + \alpha_{rs}\phi - [(\alpha_w)\phi']' - (Nr_0^2\phi')' = 0 \tag{60}$$

Substituting $\phi = \varphi \sin(n\pi s/L)$ into (60) leads to the torsional buckling load

$$P_{s\theta n\alpha} = -N = \frac{1}{r_0^2}\left[\frac{\Theta^2 EI_y}{(n\pi)^2} + \left(GJ + \frac{(n\pi)^2 EI_w}{L^2}\right) + \frac{\alpha_{rs}L^2}{(n\pi)^2} + \alpha_w\right] \tag{61}$$

which can be reduced to the torsional buckling load of a doubly symmetric column about its shear centre axis given by (Trahair, 1993)

$$P_{sn\alpha} = \frac{1}{r_0^2}\left[\left(GJ + \frac{(n\pi)^2 EI_w}{L^2}\right) + \frac{\alpha_{rs}L^2}{(n\pi)^2} + \alpha_w\right] \tag{62}$$

The lowest torsional buckling load of an unrestrained column corresponds to a single half sine wave. However, the first mode torsional buckling load of an unrestrained arch is not necessarily the lowest one. Again, the lowest torsional buckling load $P_{s\theta n}$ of an unrestrained arch in uniform compression can be determined by calculating successive values of $P_{s\theta n}/P_s$ with the number of half sine waves $n = 1, 2, 3, \ldots$, where $P_{s\theta n}$ is given by (61) with $\alpha_{rs} = \alpha_w = 0$. In general, the values of $P_{s\theta n}/P_s$ will decrease at first until the minimum is reached and then increase as shown in Fig. 14(c). Thus the successive calculation may be terminated when there is an increase in $P_{s\theta n}/P_s$.

When the length L is constant, the lowest torsional buckling load $P_{s\theta n}$ of an unrestrained arch in uniform compression increases with an increase of the included angle Θ as shown in Fig. 14(d). It can also be seen that the number of half sine waves n during torsional buckling increases with an increase of the included angle Θ.

5.4. Effects of torsional and warping restraints

The lowest flexural-torsional buckling load of an arch in uniform compression restrained by continuous torsional and warping restraints corresponds to a single half sine wave ($n = 1$) (Trahair, 1993) and the equation for the buckling load can be obtained from (54) as

$$A_3\left(\frac{P_{\theta\alpha}}{P_y}\right)^2 + B_3\left(\frac{P_{\theta\alpha}}{P_y}\right) + C_3 = 0 \tag{63}$$

where

$$A_3 = \frac{P_y}{P_s} \tag{64}$$

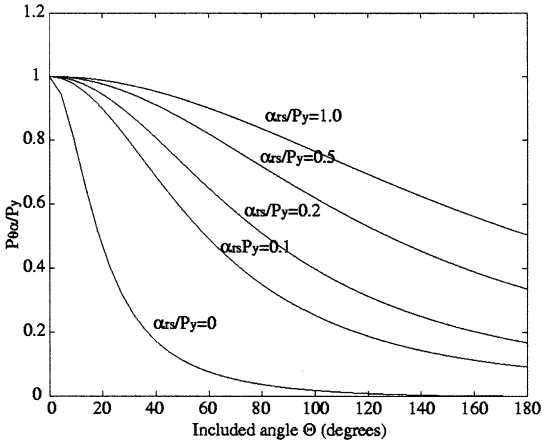

Fig. 15. Flexural-torsional buckling of arches in uniform compression with continuous torsional restraints.

$$B_3 = -\left\{1 + \frac{a^2}{b^2} + \frac{P_y}{P_s}\left(1 - a^2\right)^2 + \left(1 + \frac{r_0^2}{R^2}\right)\frac{\alpha_{\mathrm{rs}}(L/\pi)^2 + \alpha_{\mathrm{w}}}{r_0^2 P_s}\right\} \tag{65}$$

and

$$C_3 = (1 - a^2)^2 + (1 + a^2 b^2)\frac{\alpha_{\mathrm{rs}}(L/\pi)^2 + \alpha_{\mathrm{w}}}{r_0^2 P_s} \tag{66}$$

Variations of the dimensionless buckling load $P_{\theta\alpha}/P_y$ with the included angle Θ are shown in Fig. 15 for different values of the torsional restraining stiffness α_{rs}/P_y. It can be seen that the buckling load $P_{\theta\alpha}/P_y$ increases with an increase in the restraining stiffness α_{rs}/P_y, except that the torsional restraint does not affect the flexural buckling load of a column ($\Theta = 0°$). Torsional restraints are more effective for arches with a larger included angle than for arches with a smaller included angle.

5.5. Effects of minor axis rotational restraints

The lowest flexural-torsional buckling load of a column in uniform compression restrained by continuous minor axis rotational restraints corresponds to a single half sine wave (Trahair and Bradford, 1998). However, an arch restrained by continuous minor axis rotational restraints may buckle in n half sine waves, and the equation for the flexural-torsional buckling load can be obtained from (54) as

$$A_4\left(\frac{P_{\theta n\alpha}}{P_{yn}}\right)^2 + B_4\left(\frac{P_{\theta n\alpha}}{P_{yn}}\right) + C_4 = 0 \tag{67}$$

where

$$A_4 = \frac{P_{yn}}{P_{sn}} \tag{68}$$

$$B_4 = -\left\{1 + \frac{a_n^2}{b_n^2} + \frac{P_{yn}}{P_{sn}}\left(1 - a_n^2\right)^2 + \frac{\alpha_{\mathrm{ry}}}{P_{sn}}\left[\left(1 - \frac{y_{\mathrm{t}}}{R}\right)^2 + \frac{y_{\mathrm{t}}^2}{r_0^2}\right]\right\} \tag{69}$$

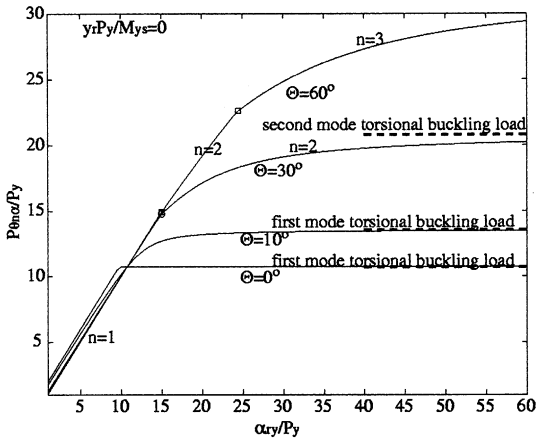

Fig. 16. Flexural-torsional buckling of arches in uniform compression with continuous minor axis rotational restraints.

and

$$C_4 = (1 - a_n^2)^2 + \frac{\alpha_{ry}}{P_{yn}}\left[\left(\frac{a_n}{b_n} - \frac{y_r P_{yn}}{M_{ysn}}\right)^2 + \left(1 - \frac{y_t}{R}\right)^2\right] \tag{70}$$

The lowest buckling load $P_{\theta n\alpha}$ for a given restraining stiffness α_{ry} acting at a height y_r may be determined in the same way as for arches in uniform bending restrained by continuous minor axis rotational restraints as discussed above.

Variations of the dimensionless buckling load $P_{\theta n\alpha}/P_y$ with the dimensionless restraint α_{ry}/P_y acting at $y_r = 0$ obtained from (67) are shown in Fig. 16 for arches with different included angle Θ. As the restraining stiffness α_{ry}/P_y increases, the buckling load $P_{\theta n\alpha}/P_y$ of the arch increases until the value of the torsional buckling load of the arch given by (61) is reached at a limiting value of the minor axis rotational restraining stiffness α_{ry}. At this stage, the buckling mode of the arch may change from flexural-torsional to torsional. To determine the limiting value of the restraining stiffness α_{ry}, the lowest torsional buckling load of the arch given by (61) and the corresponding number of half sine waves n need to be found first. The value of α_{ry} can then be found by equating the corresponding buckling load $P_{\theta n\alpha}$ of the arch obtained from (67) to the lowest torsional buckling load $P_{s\theta n}$ that is found. Further increases of the restraining stiffness α_{ry}/P_y do not increase the buckling resistance as shown in Fig. 16. The buckling resistance of the arch remains at the value of the torsional buckling load.

Variations of the dimensionless buckling load $P_{\theta\alpha}/P_y$ with the dimensionless restraint height $y_r P_y/M_{ys}$ obtained from (67) when the dimensionless restraining stiffness is constant at $\alpha_{ry}/P_y = 10$ are shown in Fig. 17 for arches with different included angles $\Theta = 0$–$150°$. Minor axis rotational restraints are more effective for arches with a larger included angle Θ than for arches with a smaller included angle Θ. The most effective height $y_r P_y/M_{ys}$ of the minor axis restraint moves from the shear centre ($y_r = 0$) for a column ($\Theta = 0°$) to above the shear centre as the included angle Θ of the arch increases. As the restraint height $y_r P_y/M_{ys}$ moves further above the most effective height, the buckling load of an arch decreases rapidly. Minor axis rotational restraints acting below the shear centre ($y_r P_y/M_{ys} > 0$) are comparatively ineffective. The number of half sine waves n corresponding to the buckling load firstly increases as the restraint height moves from below the shear centre toward to the shear centre and then decreases as the restraint height moves further above the shear centre.

Variations of the dimensionless buckling load $P_{\theta\alpha}/P_y$ with the dimensionless restraint height $y_r P_y/M_{ys}$ obtained from (67) for an arch with an included angle $\Theta = 30°$ are shown in Fig. 18 for different restraining

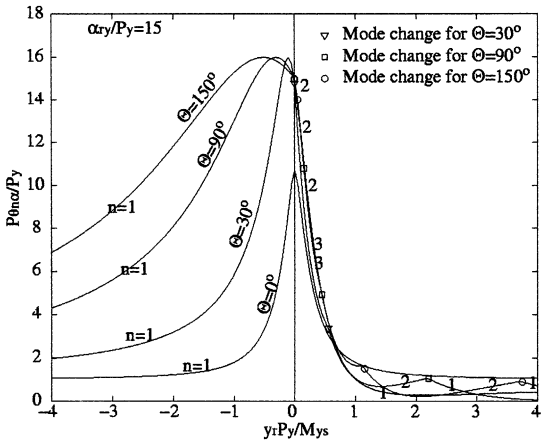

Fig. 17. Effect of restraint height on buckling of arches in uniform compression with continuous minor axis rotational restraints.

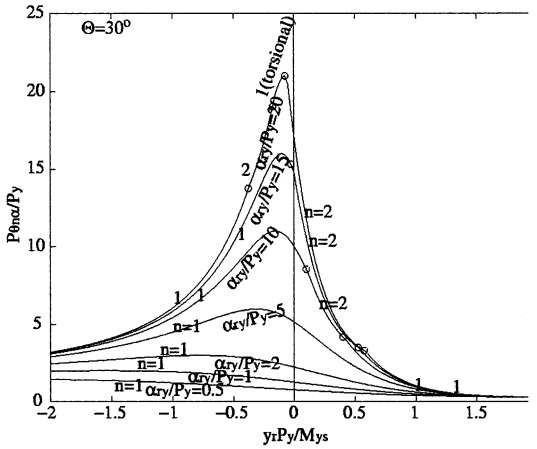

Fig. 18. Effect of restraining stiffness on buckling of arches in uniform compression with continuous minor axis rotational restraints.

stiffness α_{ry}/P_y. The lowest buckling load of the restrained arch increases significantly as the restraining stiffness increases from $\alpha_{ry}/P_y = 0.5$ to 20. The corresponding number of half sine waves n also increases with the restraining stiffness α_{ry}/P_y. When the restraining stiffness α_{ry}/P_y is higher than the corresponding limiting value (for example when $\alpha_{ry}/P_y = 20$ and $-0.05 \geqslant y_r P_y/M_{ys} \geqslant -0.15$), the buckling mode changes from flexural-torsional to torsional.

5.6. Effects of lateral-translational restraints

Arches with continuous lateral-translational restraints may buckle in n half sine waves, and the equation for the flexural-torsional buckling load can be obtained from (54) as

$$A_5\left(\frac{P_{\theta n\alpha}}{P_{yn}}\right)^2 + B_5\left(\frac{P_{\theta n\alpha}}{P_{yn}}\right) + C_5 = 0 \tag{71}$$

where

$$A_5 = \frac{P_{yn}}{P_{sn}} \tag{72}$$

$$B_5 = -\left\{1 + \frac{a_n^2}{b_n^2} + \frac{P_{yn}}{P_{sn}}\left(1 - a_n^2\right)^2 + \frac{\alpha_t (L/n\pi)^2}{P_{sn}}\left[\left(1 - \frac{y_t}{R}\right)^2 + \frac{y_t^2}{r_0^2}\right]\right\} \tag{73}$$

and

$$C_5 = (1 - a_n^2)^2 + \frac{\alpha_t (L/n\pi)^2}{P_{yn}}\left[\left(\frac{a_n}{b_n} - \frac{P_{yn} y_t}{M_{ysn}}\right)^2 + \left(1 - \frac{y_t}{R}\right)^2\right] \tag{74}$$

The lowest buckling load $P_{\theta n\alpha}$ for a given value of $\alpha_t (L/\pi)^2 P_y$ and $y_t P_y / M_{ys}$ may be determined in the same way as for arches with minor axis rotational restraint in uniform bending as discussed above.

Variations of the dimensionless buckling load $P_{\theta n\alpha}/P_y$ with the dimensionless restraining stiffness $\alpha_t (L/\pi)^2 / P_y$ acting at $y_t = 0$ are shown in Fig. 19 for arches with different included angle Θ. The number of half sine waves n corresponding to the lowest buckling load increases with an increase of the included angle Θ. As the restraining stiffness $\alpha_t (L/\pi)^2 / P_y$ increases, the flexural-torsional buckling load $P_{\theta\alpha}/P_y$ increases until the value of the torsional buckling load of an arch in uniform compression given by (61) is reached at a limiting value of the stiffness of the lateral-translational restraint $\alpha_t (L/\pi)^2 / P_y$. The limiting value of the restraining stiffness $\alpha_t (L/\pi)^2 / P_y$ can be determined in the same way as that for arches restrained by minor axis rotational restraint.

Variations of the dimensionless buckling load $P_{\theta\alpha}/P_y$ with the dimensionless restraint height $y_t P_y / M_{ys}$ obtained from (71) for specified values of the dimensionless restraining stiffness $\alpha_t (L/\pi)^2 / P_y = 20$ are shown in Fig. 20 for arches with different included angle $\Theta = 0$–$150°$. Restraints are more effective for arches with a larger included angle Θ than for arches with a smaller included angle Θ. The most effective height $y_t P_y / M_{ys}$ of the lateral-translational restraint moves from the shear centre ($y_t = 0$) for a column ($\Theta = 0°$) to above the shear centre as the included angle Θ of the arch increases. As the restraint height $y_t P_y / M_{ys}$ moves further above the most effective height, the buckling load of an arch decreases rapidly. Lateral-translational restraints acting below the shear centre ($y_r P_y / M_{ys} > 0$) are comparatively ineffective. The number of half sine waves n corresponding to the buckling load firstly increases as the restraint height y_t moves from below the

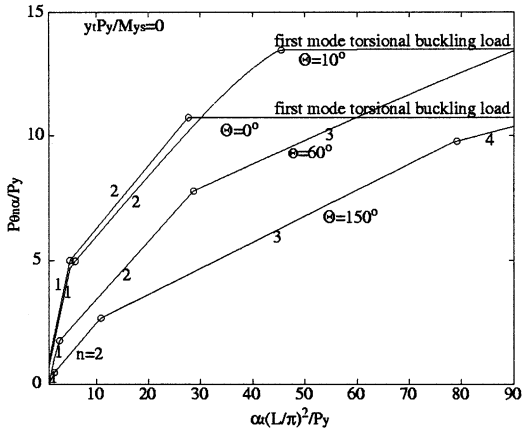

Fig. 19. Flexural-torsional buckling of arches in uniform compression with lateral-translational restraints.

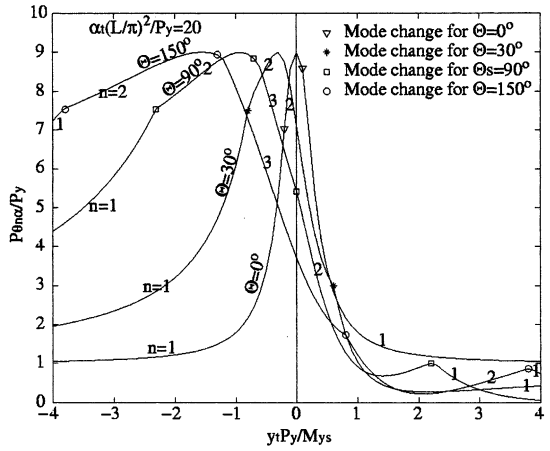

Fig. 20. Effect of restraint height on buckling of arches in uniform compression with lateral-translational restraints.

shear centre toward to the shear centre and then decreases as the restraint height y_t moves further above the shear centre.

6. Conclusions

The research presented in this paper developed and used an energy method of analysis to study the effects of continuous elastic restraints on the elastic flexural-torsional buckling of arches of doubly symmetric open thin-walled cross-section in uniform bending and in uniform compression. Closed form solutions for the flexural-torsional buckling moment of restrained arches in uniform bending and for the flexural-torsional buckling load of restrained arches in uniform compression were obtained. The closed form solutions for torsional buckling moment of restrained arches in uniform bending and for torsional buckling and flexural buckling loads of restrained arch in uniform compression were also obtained. It can be concluded that

1. Continuous elastic restraints are more effective for arches with a larger included angle than for arches with a smaller included angle.
2. When an arch in uniform bending or in uniform compression is restrained by continuous torsional and/or warping restraints, the lowest buckling resistance of the arch corresponds to the first mode buckling resistance.
3. However, when an arch in uniform bending or in uniform compression is restrained by lateral-translational and/or minor axis rotational restraints, the first mode buckling resistance may not correspond to the lowest buckling resistance of the arch and the number of half sine waves corresponding to the lowest buckling resistance increases with an increase in the stiffness of the restraints.
4. For an arch in uniform bending and restrained by the lateral-translational and/or minor axis rotational restraints, when the stiffness of the restraints approaches infinity, the buckling mode of the arch changes from being flexural-torsional to torsional about an enforced centre of rotation. However, for arches in uniform compression and restrained by the lateral-translational and/or minor axis rotational restraints, when the stiffness of the restraints approaches a limiting value instead of infinity, the buckling mode of the arch changes from being flexural-torsional to torsional.
5. For an arch in uniform bending or in uniform compression and restrained by the lateral-translational and/or minor axis rotational restraints, when the stiffness and height of the restraints are constant,

the lowest buckling resistance and the corresponding number of half sine waves increase with the included angle of the arch.

6. For an arch in uniform bending and restrained by the lateral-translational and/or minor axis rotational restraints, as the restraint position moves from below the shear centre to above the shear centre, the lowest buckling moment and the corresponding number of half sine waves increase. Restraints below the shear centre are comparatively ineffective.
7. For an arch in uniform compression and restrained by the lateral-translational and/or minor axis rotational restraints, as the restraint position moves from below the shear centre toward above the shear centre, the lowest buckling load and the corresponding number of half sine waves increase first and then decrease. Restraints away from the shear centre are ineffective.

Acknowledgements

This work has been supported by a research grant awarded to the second author by the Australian Research Council under the ARC Large Grants Scheme.

References

Bradford, M.A., 1989. Buckling of beams supported on seats. The Structural Engineer 67 (23), 411–414.

Helwig, T.A., Yura, J.A., 1999. Torsional bracing of columns. Journal of Structural Engineering ASCE 125 (5), 547–555.

Mutton, B.R., Trahair, N.S., 1973. Stiffness requirements for lateral bracing. Journal of the Structural Division ASCE 99 (ST10), 2167–2182.

Nethercot, D.A., 1973. Buckling of laterally and torsionally restrained beams. Journal of the Engineering Mechanics Division ASCE 99 (EM4), 773–791.

Ojalvo, M., Chambers, R.S., 1977. Effect of warping restraints on I-beam buckling. Journal of the Structural Division ASCE 103 (ST12), 2351–2360.

Papangelis, J.P., Trahair, N.S., 1987. Flexural-torsional buckling of arches. Journal of Structural Engineering ASCE 113 (4), 889–906.

Pi, Y.-L., Bradford, M.A., 2001. Elastic flexural-torsional buckling of restrained arches. UNICIV Report no. R-398. School of Civil and Environmental Engineering, The University of New South Wales, Sydney.

Pi, Y.-L., Trahair, N.S., 1996. Three-dimensional analysis of elastic arches. Engineering Structures 18 (1), 49–63.

Pi, Y.-L., Papangelis, J.P., Trahair, N.S., 1995. Prebuckling deformations and flexural-torsional buckling of arches. Journal of Structural Engineering ASCE 121 (9), 1313–1322.

Rajasekaran, S., Padmanabhan, S., 1989. Equations of curved beams. Journal of Engineering Mechanics ASCE 115 (5), 1094–1111.

Svensson, S.E., Plum, C.M., 1983. Stiffener effects on torsional buckling of columns. Journal of Structural Engineering ASCE 109 (3), 758–772.

Taylor, A.C., Ojalvo, M., 1966. Torsional restraint of lateral buckling. Journal of the Structural Division ASCE 92 (ST2), 115–129.

Trahair, N.S., 1993. Flexural-torsional Buckling of Structures. E & FN Spon, London.

Trahair, N.S., Bradford, M.A., 1998. The Behaviour and Design of Steel Structures to AS4100, Third Australian edition. E & FN Spon, London.

Timoshenko, S.P., Gere, J.M., 1961. Theory of Elastic Stability, Second edition. McGraw-Hill, New York.

Valentino, J., Trahair, N.S., 1998. Torsional restraint against elastic lateral buckling. Journal of Structural Engineering ASCE 124 (10), 1217–1226.

Vlasov, V.Z., 1961. Thin-walled Elastic Beams, Second edition. Israel Program for Scientific Translation, Jerusalem.

Winter, G., 1958. Lateral bracing of columns and beams. Journal of the Structural Division ASCE 84 (ST2), 1561.1–1561.22.

Yang, Y.-B., Kuo, S.-R., 1987. Effect of curvature on stability of curved beams. Journal of Engineering Mechanics ASCE 113 (6), 821–841.

Yura, J.A., 1993. Fundamentals of beam bracing. In: Proceedings of the Structural Stability Research Council Conference, Milwaukee, SSRC, pp. 1–19.